Electronic Supplementary Information for

A smart sensing triazine hexacarboxylic metal-organic skeleton material: synthesis, structure and multifunctional fluorescence detector

Yao Xiao[a], Bing Li[a], Zi Xin You[a], Yong Heng Xing[a], Feng Ying Bai[a]*, Li-Xian Sun[b] and Zhan Shi[c]*

[a] College of Chemistry and Chemical Engineering, Liaoning Normal University, Huanghe Road 850#, Dalian 116029, P. R. China.

[b] Guangxi Key Laboratory of Information Materials, Guilin University of Electronic Technology, Guilin 541004, P. R. China.

[c] State Key Laboratory of Inorganic Synthesis and Preparative Chemistry, College of Chemistry, Jilin University, Changchun 130012, P.R. China.

Contents

Materials and methods

Scheme 1 Synthetic route of ligand H_6TDPAT.

Table S1 Single crystal structure data for the complex **1**.

Table S2 Selected Bond Lengths (Å) for Complex **1**.

Table S3 IR data of complex **1** and ligand H_6TDPAT (cm^{-1}).

Table S4 UV-vis spectrum identifications of complex **1** and ligand H_6TDPAT.

Table S5 The lifetime of complex 1 in different organic solvents.

Table S6 The fluorescence quantum yields of complex **1** in different solvents.

Figure S1 AFM images at different reaction times.

Figure S2 IR spectra of H_6TDPAT and complex **1**.

Figure S3 The UV-vis spectra of H_6TDPAT and complex **1**.

Figure S4 PXRD spectra of complex**1**.

Figure S5 The TG curve of complex **1**.

Figure S6 Interference experiment of different ions on the detection of Fe^{3+} by complex **1**.

Figure S7 Stern-Volmer fitting linear of MnO_4^- and $Cr_2O_7^{2-}$.

Figure S8 Interference experiment of different ions on the detection of MnO_4^- and $Cr_2O_7^{2-}$ by complex **1**.

Figure S9 The S-V fitting plot for complex **1** of detecting MPDA.

Figure S10 UV-Vis absorption spectrum of complex **1** and the detected substance.

Figure S11 Fluorescence sensing response and K_{sv} values of ligand H_6TDPAT to different substances.

Figure S12 The lifetime curve of complex **1**.

Figure S13 Fluorescence lifetime of complex **1** after adding other detection substances at low concentrations and at high concentrations, respectively.

Figure S14 The fluorescence lifetime of complex 1 before and after detecting $Cr_2O_7^{2-}$.

Materials and Methods.

The ligand H_6TDPAT was prepared by literature method and appropriately modified the methods [1]. The synthetic route is shown in Scheme 1. All other original chemical reagents and solvents employed in the present work were purchased from commercial sources and used without further purification. The Bruker AXS TENSOR-27 FT-IR spectrometer was applied to record Infrared spectra in the range of 4000-400 cm^{-1}. UV-vis absorption spectra of solid sample were received from a JASCO V-570 UV/VIS/NIR spectrophotometer with the range of 200-800 nm, and Lambda 35 spectrometer was applied to record the UV-vis absorption spectra of suspension samples in 200-800 nm. Thermogravimetric data was obtained from a PerkinElmer Diamond TG/DTA under nitrogen protection from room temperature to 1100 °C with the heating rate of 10 ℃ •min^{-1}. X-ray powder diffraction (PXRD) patterns were performed on an Advance D8 equipped with Cu-Kα radiation in the range of 5° < 2θ < 60°, with a step size of 0.02° (2θ) and a count time of 2 s per step. The HORIBA Fluoromax-4-TCSPC spectrofluorometer which is provided with Pulsed LED sources (200-1000 nm) with 3.2-inch Integrating Sphere was used to measure the fluorescence behavior of the coordination complexes at room temperature. The size and morphology of the material surface was investigated by Scanning Electron Microscope & X-ray Analyzer (SEM, SU8010) and Atomic Force Microscope (AFM, Asylum Research Cypher ES).

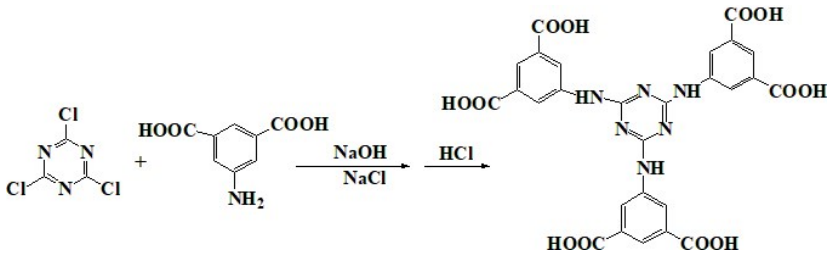

Scheme 1 Synthetic route of ligand H_6TDPAT

Table S1 Single crystal structure data for the complex **1**

Complex 1	Before squeeze	After squeeze
Formula	$C_{54}H_{24}N_{12}O_{25.5}Tb_3$	$[(NH_2(Me)_2^+]_3 \cdot [Tb_3(TDPAT)_2(H_2O)_{1.5}] \cdot 3EtOH \cdot 24H_2O$
M (g mol^{-1})	1725.65	1725.65
crystal system	cubic	cubic
space group	$I23$	$I23$
a (Å)	27.6250(6)	27.6250(6)
b (Å)	27.6250(6)	27.6250(6)
c (Å)	27.6250(6)	27.6250(6)
α (deg)	90	90
β (deg)	90	90
γ (deg)	90	90
V ($Å^3$)	21267(2)	21267(2)
Z	8	8
D_{calc} ($g \cdot cm^{-3}$)	1.551	1.551

F(000)	10008	10008
μ(Mo–Kα) (mm^{-1})	2.063	2.063
θ (deg)	1.04 - 28.07	1.04 - 28.07
Reflections collected	68160	68160
independent reflections (I>2σ(I))	8640	8640
Parameters	285	285
Δ(ρ) (e Å^{-3})	0.795 and -0.447	0.795 and -0.447
goodness of fit on F^2	1.017	1.017
R [a]	0.0259 (0.0303)[b]	0.0259 (0.0303)[b]
wR_2 [a]	0.0614 (0.0625)[b]	0.0614 (0.0625)[b]

[a] $R=\Sigma||F_o|-|F_c||/\Sigma|F_o|$, $wR_2=(\Sigma(w(F_o^2-F_c^2)^2/\Sigma(w(F_o^2)^2)^{1/2}$; [$F_o$>4σ($F_o$)]; [b] based on all data

Table S2 Selected Bond Lengths (Å) for Complex **1**

Complex 1			
Tb(1)-O(1)	2.474(3)	Tb(1)-O(1#)	2.584(3)
Tb(1)-O(2)	2.462(3)	Tb(1)-O(3)	2.273(2)
Tb(1)-O(4)	2.438(3)	Tb(1)-O(5)	2.490(3)
Tb(1)-O(6)	2.255(3)	Tb(1)-O(8)	2.258(3)

Table S3 IR data of complex **1** and ligand H_6TDPAT (cm^{-1})

	Complex	H_6TDPAT
$\nu_{(N-H)}$	3583	3433
$\nu_{(Ar-H)}$	3106	3188
$\nu_{(CH2)}$	2950,2856	2933, 2845
$\nu_{(C=N)}$	1532	1528
$\nu_{(C=C)}$	1598	1572
$\nu_{(ascoo-)}$	1707	1623
$\nu_{(scoo-)}$	1412	1378
$\nu_{(C-N)}$	1187	1115
$\nu_{(C-O)}$	1077	1026
$\delta_{(Ar-H)}$	933,774	904,798
$\nu_{(Ln-O)}$	-	614

Table S4 UV-vis spectrum identifications of complex **1** and ligand H_6TDPAT

Complex	Wavelength(nm)	Transition	Types
H_6TDPAT	217, 265	π-π*	
	347	n-π*	
1	267	π-π*	LLCT
	330	n-π*	LLCT
	463	O-Tb	LMCT

Table S5 The lifetime of complex 1 in different organic solvents

Solvents	Lifetime (s)	Average Lifetime (s)
Complex **1**	$\tau1=2.042871\times10^{-5}$ $\tau2=3.485968\times10^{-6}$	$T=8.489039\times10^{-4}$
DMA	$\tau1=1.825785\times10^{-6}$ $\tau2=2.064967\times10^{-6}$	$T=1.07975\times10^{-3}$
DMF	$\tau1=1.802947\times10^{-6}$ $\tau2=2.052005\times10^{-6}$	$T=1.085945\times10^{-3}$
CH_2Cl_2	$\tau1=1.69563\times10^{-6}$ $\tau2=1.624757\times10^{-6}$	$T=9.987784\times10^{-4}$
MeOH	$\tau1=1.699469\times10^{-6}$ $\tau2=1.761614\times10^{-6}$	$T=1.022173\times10^{-3}$
EtOH	$\tau1=1.691361\times10^{-6}$ $\tau2=1.911976\times10^{-6}$	$T=1.080233\times10^{-3}$
MeCN	$\tau1=1.810699\times10^{-6}$ $\tau2=2.052299\times10^{-6}$	$T=1.099839\times10^{-3}$
EA	$\tau1=9.50361\times10^{-7}$	$T=1.014549\times10^{-3}$
N-hexane	$\tau1=1.648482\times10^{-6}$ $\tau2=1.74622310^{-6}$	$T=1.03164\times10^{-3}$
H_2O	$\tau1=2.625532\times10^{-6}$ $\tau2=1.136978\times10^{-6}$	$T=7.427649\times10^{-4}$

Table S6 The fluorescence quantum yields of complex **1** in different organic solvents

Solvents	Quantum yields
DMA	43.54
DMF	43.45
CH_2Cl_2	40.05
MeOH	55.76
EtOH	44.55
MeCN	54.61
EA	50.49
N-hexane	39.81
H_2O	40.88

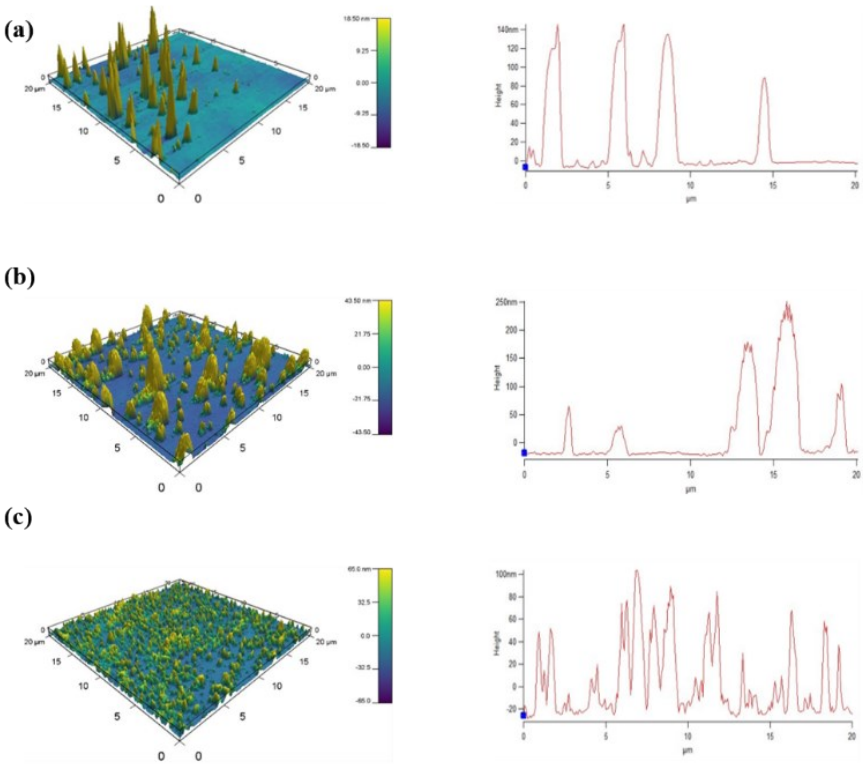

Figure S1 AFM images at different reaction times：(a) before the reaction; (b) during the reaction;(c) after the reaction

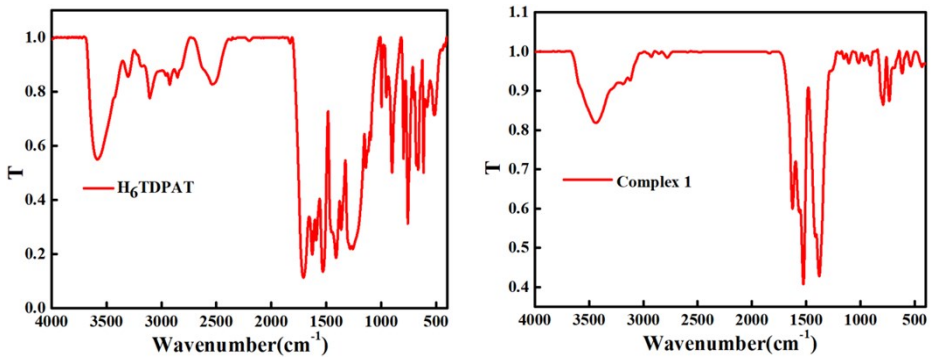

Figure S2 IR spectra of H_6TDPAT and complex **1**

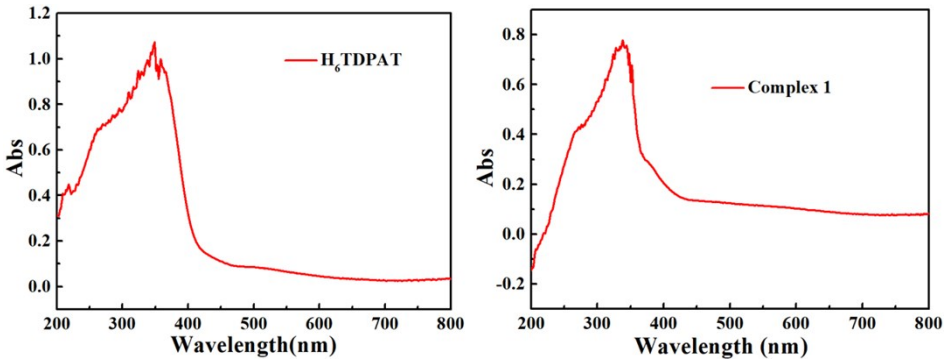

Figure S3 The UV-vis spectra of H_6TDPAT and complex **1**

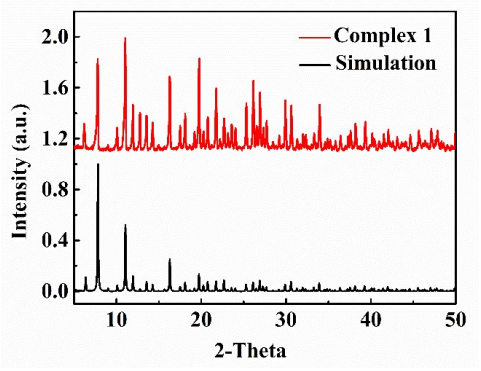

Figure S4 PXRD spectra of complex **1**

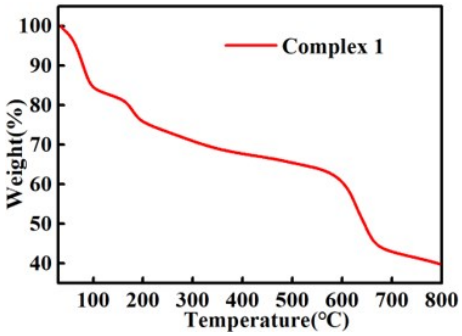

Figure S5 The TG curve of complex **1**

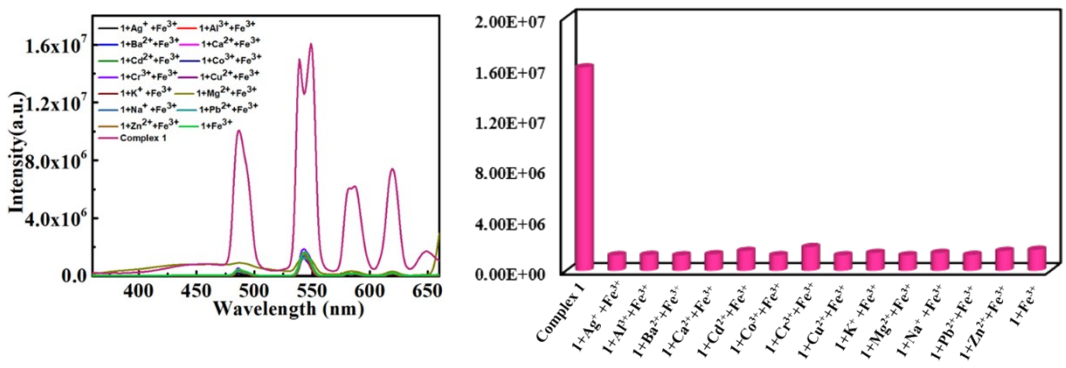

Figure S6 (a) The change of fluorescent spectra of the complex **1** interacting with different metal ions with and without Fe^{3+} ions (b) The change of fluorescent spectra at 543 nm of the complex **1** interacting with different metal ions with and without Fe^{3+} ions.

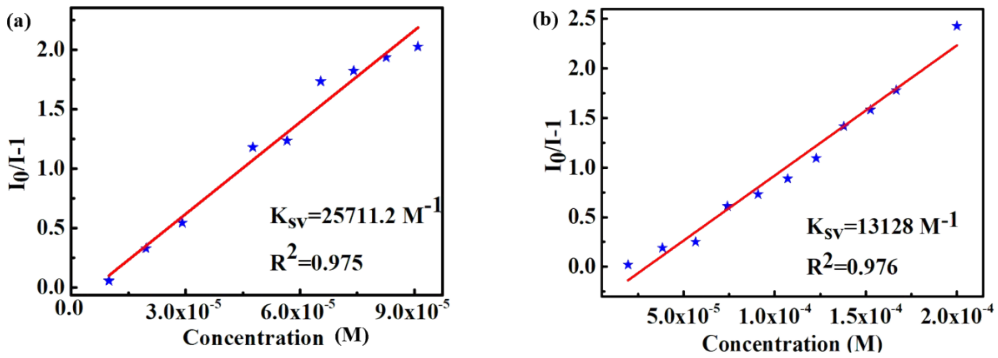

Figure S7 Stern-Volmer fitting linear plot of (a) MnO_4^- (10^{-3}mol/L) detected by complex **1**; (b) Stern-Volmer fitting linear plot of $Cr_2O_7^{2-}$ (10^{-3}mol/L) detected by complex **1**

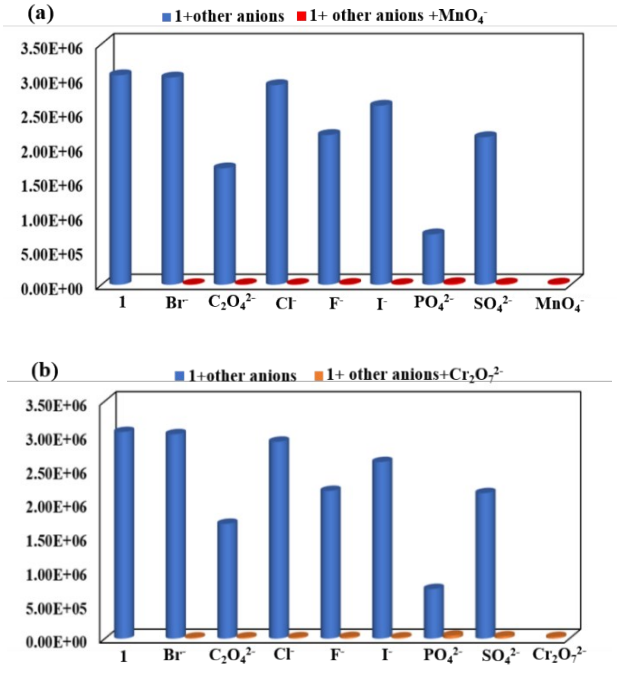

Figure S8 The change of luminescence intensities of complex **1** at 543 nm upon addition of anions: (a) $Cr_2O_7^{2-}$, (b) MnO_4^-

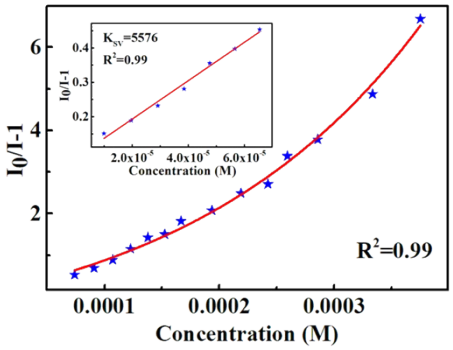

Figure S9 The S-V fitting plot for complex **1** of detecting MPDA

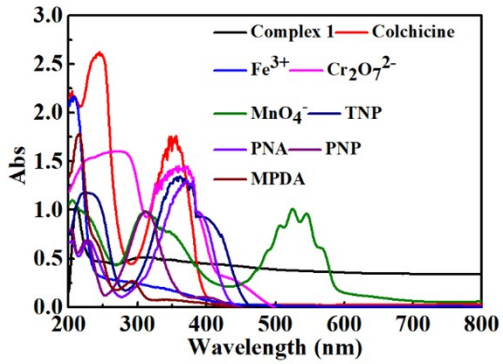

Figure S10 UV-Vis absorption spectrum of complex **1** and the detected substance

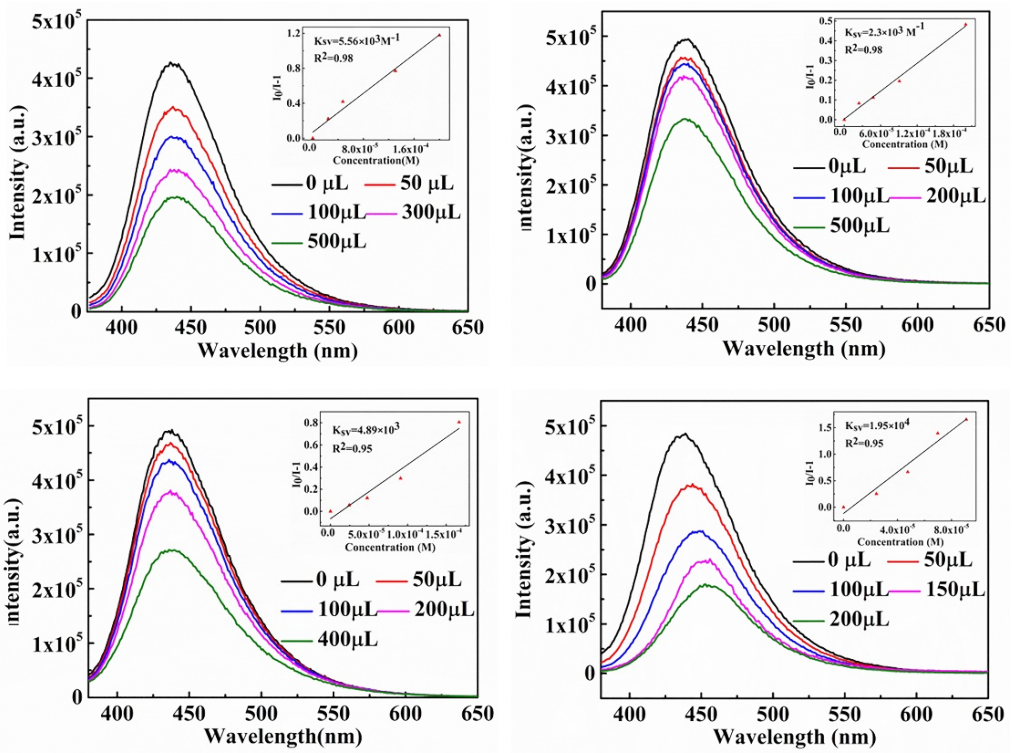

Figure S11 Fluorescence sensing response and K_{sv} values of ligand H_6TDPAT to different substances: (a) Colchicine (b) Fe^{3+} (c) MnO_4^-(d) TNP

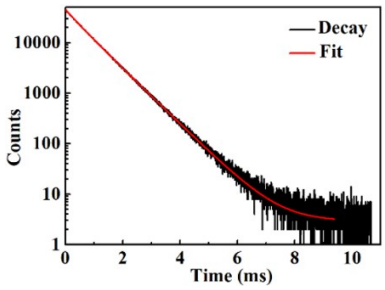

Figure S12 The lifetime curve of complex **1**

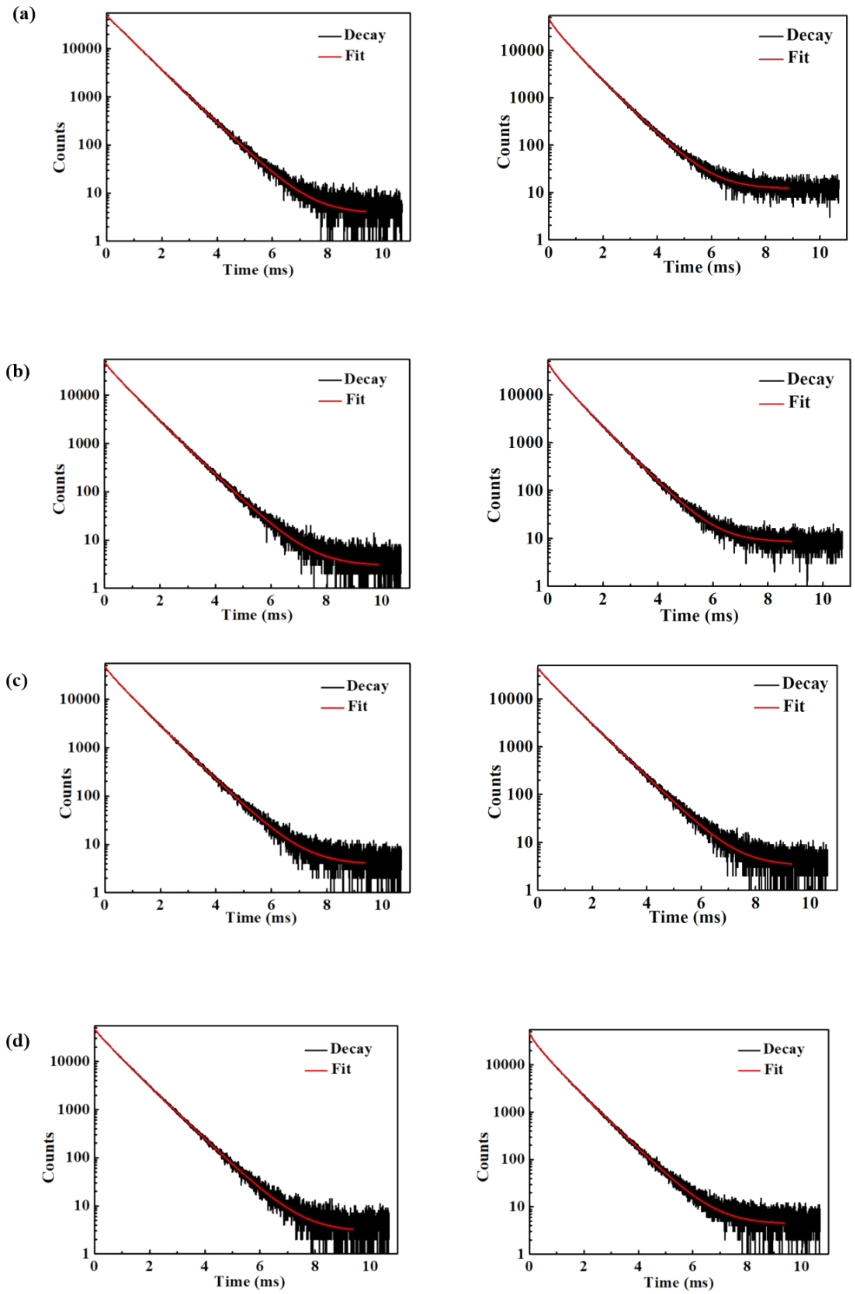

Figure S13 Fluorescence lifetimes of complex **1** after adding other detection substances at low concentrations and at high concentrations, respectively: (a) colchicine, (b)Fe^{3+}, (c)TNP and (d) MPDA

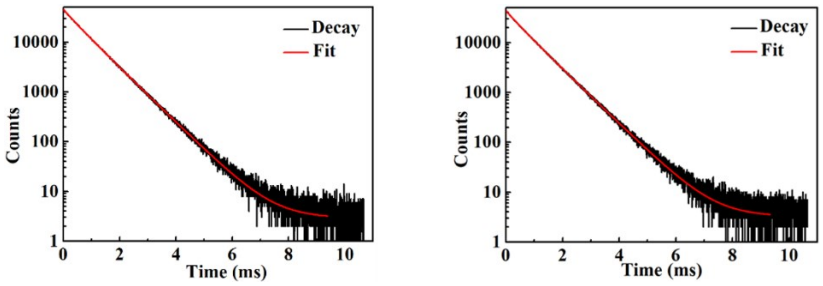

Figure S14 The fluorescence lifetime of complex **1** before and after detecting $Cr_2O_7^{2-}$

References

[1] B Li, Z J Zhang,Y Li, K X Yao, Y H Zhu, Z Y Deng, F Yang, X J Zhou, G H Li, H H Wu, N Nijem, Y J Chabal, Z P Lai, Y Han, Shi Z, S H Feng and J Li, Angew Chem Int Ed Engl, 2012, 124(6):1441-1444.